Effective Capacity Analysis for Underlay Cognitive Satellite-Terrestrial Networks

Yuhan Ruan*, Yongzhao Li*[1], Cheng-Xiang Wang†, Rui Zhang*, and Hailin Zhang*
*State Key Laboratory of Integrated Service Network, Xidian University, Xi'an, 710071, China
†School of Engineering and Physical Sciences, Heriot-Watt University, Edinburgh, EH14 4AS, UK
E-mail:{ryh911228@163.com, Cheng-Xiang.Wang@hw.ac.uk, rui_zhang_xd@163.com, hlzhang@xidian.edu.cn}
[1]Corresponding author: yzhli@xidian.edu.cn

***Abstract*—In this paper, we consider a cognitive satellite-terrestrial network where the satellite communication operates in the microwave frequency bands allocated to terrestrial networks in an underlay mode. Taking the statistical delay quality-of-service (QoS) requirements into account, we investigate the effective capacity of the satellite network while satisfying interference-power limitations imposed by terrestrial networks. Specifically, the primary terrestrial transmitters that would result in aggregate interference at the satellite receiver are modeled as points of a Poisson point process (PPP). By characterizing the aggregate interference as a gamma distribution, we obtain a closed-form expression for the effective capacity of the secondary satellite network. Finally, simulation results are provided to not only demonstrate the validity of the theoretical results, but also show the effects of system parameters such as delay exponent of satellite communications, interference-power limitations of terrestrial networks, and intensity of terrestrial transmitters on the performance of the satellite network.**

***Index Terms*—Underlay cognitive satellite-terrestrial networks, Poisson point process, delay QoS requirement, effective capacity, interference-power constraint.**

I. Introduction

Future satellite communication systems are expected to provide high data-rate broadband services. However, the limited spectral resources can hardly meet the increasing demand for satellite applications and services. To tackle this issue, cognitive radio technology has emerged as a promising solution to enhance the spectrum utilization by enabling dynamic spectrum access between satellite and terrestrial networks, referred as cognitive satellite-terrestrial networks [1], [2]. Various spectrum sharing approaches are suggested for cognitive satellite-terrestrial networks, e.g., underlay, overlay, and interweave [3]. The underlay mode is especially attractive due to its high spectral efficiency of the overall system, which allows cognitive systems to reutilize the spectrum in which incumbent signals are present as long as their interference imposed to the primary receiver is below a predefined threshold.

Until now, many works have analyzed and optimized the performance of the underlay cognitive satellite-terrestrial network. The authors in [4] and [5] maximized the satellite throughput through a carrier-power-bandwidth allocation scheme and a game-theory based scheduling algorithm, respectively. For the protection of the primary users' communication, the authors in [6] introduced a power allocation scheme for the cognitive terrestrial link while guaranteeing the outage probability (OP) of the incumbent satellite communication. Besides, the authors in [7] theoretically investigated the OP of a cognitive hybrid satellite-terrestrial relay network with interference constraints. These studies mainly concentrate on mitigating the performance degradation caused by interference, while ignoring the QoS requirements of end users. However, QoS guarantees play a critical role in future broadband satellite networks, e.g., in real-time or delay-sensitive applications, it is required to ensure that the delay adheres to the service requirements [8], [9]. In this regard, the authors in [10] optimized the performance of satellite systems from the perspective of effective capacity, which has been recently introduced by Wu and Negi [11] as a link-layer channel model for supporting QoS requirements.

The majority of the aforementioned works consider the interference management and the QoS requirements separately, failing to illustrate the coexistence of the satellite network and the terrestrial network commendably. Motivated by this, we investigate the performance of the cognitive satellite-terrestrial network in this paper, giving consideration to both networks simultaneously. From the perspective of statistical delay QoS requirements, we employ the concept of effective capacity, which is defined as the maximum constant arrival rate that can be supported by the channel under a given delay constraint. Moreover, the primary terrestrial transmitters that would result in aggregate interference at the satellite receiver are modeled as points of a PPP [12]. By characterizing the aggregate interference as a gamma distribution, we obtain a closed-form expression for the effective capacity of the secondary satellite network while satisfying interference-power limitations imposed by the primary terrestrial network. Finally, simulation results are provided to not only demonstrate the validity of the theoretical results, but also show the effects of system parameters such as delay exponent of satellite communications, interference-power limitations of primary networks, and intensity of primary transmitters on the performance of the secondary network.

The remainder of the paper is organized as follows. Section II introduces the system model. Section III presents the effective capacity analysis of the cognitive satellite-terrestrial network. Numerical and simulation results that illustrate the correctness of the analysis are given in section IV. Finally, conclusions are made in section V.

978-1-4673-8999-0/17/$31.00 ©2017 IEEE

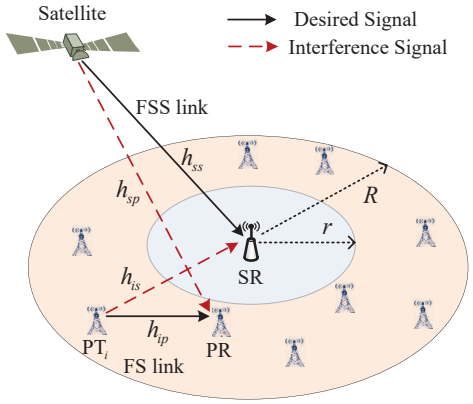

Fig. 1. Underlay cognitive satellite-terrestrial networks.

II. System Model

As shown in Fig. 1, we consider a cognitive satellite-terrestrial network where the satellite transmits signals to Fixed Satellite Service (FSS) terminals, exploiting the spectrum bands allocated to terrestrial Fixed-Service (FS) microwave links. In this case, the satellite will interfere the primary receiver (PR) while the secondary receiver (SR) will also suffer from the aggregate interference caused by N primary transmitters (PT). Considering the number and locations of PTs are random, we characterize the spatial distribution of PTs as a PPP with intensity λ. Without loss of generality, N PTs are taken to be located in a finite annular area centered around the satellite receiver. The circle with radius r is the exclusion region, which plays an important role to protect the sensitive satellite receiver from severe interference [13]. R denotes the outer radius and the interference from PTs beyond R is assumed to be negligible due to path loss.

A. Signal Model

In the considered network, the signal received at the satellite receiver can be expressed as

$$y = \sqrt{P_{\rm s}} h_{ss} x + \sum_{i=1}^{N} \sqrt{P_{\rm I}} h_{is} z + n \tag{1}$$

where x is the desired signal from satellite and z is the interference from surrounding PTs. $P_{\rm s}$ and $P_{\rm I}$ are the transmit powers of satellite and PT_i, respectively. h_{ss} and h_{is} are the channel gains of satellite $\rightarrow$ SR and $\mathrm{PT}_i \rightarrow$ PR links, respectively. n is the complex additive white Gaussian noise (AWGN) with distribution $\mathcal{CN}(0, N_0)$. The signal-to-interference-plus-noise ratio (SINR) for the satellite communication is

$$\gamma = \frac{P_{\rm s}|h_{ss}|^2}{Z + N_0} \tag{2}$$

where $Z = \sum_{i=1}^{N} P_{\rm I}|h_{is}|^2$ is the aggregate interference received at the satellite receiver. In this paper, power gain between PT_i and the satellite receiver, $|h_{is}|^2$, is assumed to be exponentially decayed with parameter α and follow a gamma distribution with a shape parameter k_{ps} and a scale parameter η_{ps}. As a result, the aggregate interference from the PPP based PTs can be approximated as a gamma distribution with a shape parameter $k_{\rm I} = \frac{(\mathrm{E}[Z])^2}{\mathrm{Var}[Z]}$ and a scale parameter $\eta_{\rm I} = \frac{\mathrm{Var}[Z]}{\mathrm{E}[Z]}$, i.e., $Z \sim \mathcal{G}(k_{\rm I}, \eta_{\rm I})$ [14], where

$$\begin{cases} \mathrm{E}[Z] = 2\pi P_{\rm I} \lambda \sqrt{\frac{k_{ps}+1}{2k_{ps}}} \left(\frac{R^{2-\alpha} - r^{2-\alpha}}{2-\alpha} \right) \\ \mathrm{Var}[Z] = \pi P_{\rm I}^2 \lambda k_{ps} (1 + k_{ps}) \eta_{ps}^2 \left(\frac{R^{2-2\alpha} - r^{2-2\alpha}}{1-\alpha} \right) \end{cases}. \tag{3}$$

To prevent the primary users from being interfered beyond an interference-power threshold I_{th} , the transmit power at the satellite should satisfy

$$P_{\rm s} = \min\left(\frac{I_{\rm th}}{|h_{sp}|^2}, P_{\rm m} \right) \tag{4}$$

where $P_{\rm m}$ denotes the maximum permitted transmit power at the satellite constrained by battery capacity. h_{sp} is the channel coefficient between the satellite and the PR with the largest elevation angle.

Based on the interference model and interference-power limitation described above, the SINR in (2) can be rewritten as

$$\gamma = \frac{\bar{\gamma}_{\rm s}|h_{ss}|^2}{\tilde{Z} + 1} \tag{5}$$

where $\bar{\gamma}_{\rm s} = P_{\rm s}/N_0 = \min\left(\bar{\gamma}_{\rm th}/|h_{sp}|^2, \bar{\gamma}_{\rm m}\right)$ denotes the average signal-to-noise ratio (SNR) with $\bar{\gamma}_{\rm th} = I_{\rm th}/N_0$ and $\bar{\gamma}_{\rm m} = P_{\rm m}/N_0$. $\tilde{Z} = Z/N_0$ denotes the ratio of the received aggregate interference to noise. From the properties of gamma distribution, we have $\tilde{Z} \sim \mathcal{G}(k_{\rm I}, \bar{\gamma}_{\rm I}\tilde{\eta}_{\rm I})$, where $\bar{\gamma}_{\rm I} = P_{\rm I}/N_0$ denotes the average interference-to-noise ratio (INR) of each terrestrial interference link and $\tilde{\eta}_{\rm I} = \eta_{\rm I}/P_{\rm I}$. So the probability density function (PDF) of $\tilde{Z}$ can be expressed as

$$f_{\tilde{Z}}(x) = \frac{x^{k_{\rm I}-1} e^{-\frac{x}{\bar{\gamma}_{\rm I}\tilde{\eta}_{\rm I}}}}{\Gamma(k_{\rm I})(\bar{\gamma}_{\rm I}\tilde{\eta}_{\rm I})^{k_{\rm I}}}. \tag{6}$$

B. Channel Model

The well-known land mobile satellite (LMS) model is the shadowed-Rician model [15], where the power of the line-of-sight (LOS) component is assumed to be gamma distributed while the multipath component has a Rayleigh distribution. Since the confluent hypergeometric function is involved in the channel model as well as the the aggregate interference from the poisson field of interferers, it is almost analytically intractable for the performance derivation of the considered network. Therefore, in this paper, we model the satellite fading channels as generalized-K distribution because of its relatively simple mathematical form that enables an integrated performance analysis of digital communication systems operating in composite multipath/shadowing fading environment [16]. The generalized-K distribution is a mixture of gamma distributed shadowing and Nakagami-distributed multipath fading. As demonstrated in [17], the generalized-K model can properly describe the channel environment of satellite communications.

For the generalized-K model, the PDF of $|h_i|^2$ $(i = ss, sp)$, can be written as

$$f_{|h_i|^2}(x) = \frac{2b^{\varphi+\varepsilon}x^{\left(\frac{\varphi+\varepsilon}{2}\right)-1}}{\Gamma(\varepsilon)\Gamma(\varphi)}K_{\varphi-\varepsilon}\left(2b\sqrt{x}\right),\ x>0 \tag{7}$$

where $K_{\varphi-\varepsilon}(\cdot)$ is the modified Bessel function of the second kind with order $(\varphi-\varepsilon)$, $b=\sqrt{\frac{\varphi\varepsilon}{\Omega_0}}$. $\varepsilon \geq 0.5$ and $\varphi \geq 0$ are the multipath parameter and shadowing parameter, respectively, and Ω_0 is the mean of the received local power.

III. Effective Capacity Analysis

In the considered network, despite the time-varying nature of satellite channels, satellite service providers must guarantee a specified QoS to satisfy their customers who have real-time multimedia traffics. For this purpose, we make use of the concept of effective capacity, which has been recently introduced by Wu and Negi [11] as the maximum constant arrival rate that a given service process can support under a given delay constraint, specified by the QoS exponent θ. In contrast to Shannon capacity without any restrictions on complexity and delay, the effective capacity ensures the maximum probabilistic delay for the incoming user traffic in the network.

In our analysis, we use the normalized effective capacity that can be expressed as

$$E_c(\theta) = -\frac{1}{\theta T_f B}\ln\left(E\left\{e^{-\theta R[i]}\right\}\right) \tag{8}$$

where $\{R[i], i=1,2,\cdots\}$ denotes the discrete-time, stationary, ergodic stochastic service process. In the following discussion, the discrete time index i is omitted for simplicity. $R = T_f B\log(1+\gamma)$ with B being the system bandwidth and T_f the fading block length. The QoS exponent θ is a positive constant which represents the decaying rate of the QoS violation probability. Note that larger θ corresponds to more strict QoS constraint, while smaller θ implies looser QoS requirement. Then the effective capacity of (8) can be derived as

$$E_c(\theta) = -\frac{1}{\theta T_f B}\ln\left(\int_0^\infty e^{-\theta T_f B\log_2(1+x)}f_\gamma(x)\,dx\right). \tag{9}$$

Considering the SINR specified in (5) involves in min-function and aggregate interference, in this paper, we prefer the moment generating function (MGF) based effective capacity analysis for its lower complexity rather than the PDF based analysis [18], i.e.,

$$E_c(\theta) = -\frac{1}{\beta\ln 2}\ln\left(\frac{1}{\Gamma(\beta)}\int_0^\infty e^{-s}s^{\beta-1}M_\gamma(s)\,ds\right) \tag{10}$$

where $\beta = \theta T_f B/\ln 2$ is the normalized QoS exponent. $\Gamma(\cdot)$ is gamma function and $M_\gamma(s) = E\{e^{-s\gamma}\} = \int_0^\infty se^{-sx}F_\gamma(x)dx$. The cumulative distribution function (CDF) of the received SINR, $F_\gamma(x)$, is given by

$$\begin{aligned} F_\gamma(x) &= \Pr\left(\bar{\gamma}_s|h_{ss}|^2 \leq x\left(\tilde{Z}+1\right)\right) \\ &= \mathrm{E}_Z\left\{F_{\bar{\gamma}_s|h_{ss}|^2}\left(x\left(\tilde{Z}+1\right)\middle|\tilde{Z}=z\right)\right\} \end{aligned} \tag{11}$$

where $\bar{\gamma}_\mathrm{s}|h_{ss}|^2 = \min\left(\bar{\gamma}_\mathrm{th}|h_{ss}|^2\middle/|h_{sp}|^2, \bar{\gamma}_\mathrm{m}|h_{ss}|^2\right)$. From the properties of min-function, the CDF of $\bar{\gamma}_\mathrm{s}|h_{ss}|^2$ can be expressed as the sum of the following probabilities, i.e.,

$$\begin{aligned} F_{\bar{\gamma}_\mathrm{s}|h_{ss}|^2}(x) = &\Pr\left(\frac{\bar{\gamma}_\mathrm{th}|h_{ss}|^2}{|h_{sp}|^2} \leq x, \frac{\bar{\gamma}_\mathrm{th}}{|h_{sp}|^2} \leq \bar{\gamma}_\mathrm{m}\right) \\ &+ \Pr\left(\bar{\gamma}_\mathrm{m}|h_{ss}|^2 \leq x, \frac{\bar{\gamma}_\mathrm{th}}{|h_{sp}|^2} > \bar{\gamma}_\mathrm{m}\right). \end{aligned} \tag{12}$$

Then, employing the concept of CDF, $F_{\bar{\gamma}_\mathrm{s}|h_{ss}|^2}(x)$ can be further deduced as

$$\begin{aligned} F_{\bar{\gamma}_\mathrm{s}|h_{ss}|^2}(x) = &\underbrace{\int_0^{\bar{\gamma}_\mathrm{th}/\bar{\gamma}_\mathrm{m}} F_{|h_{ss}|^2}\left(\frac{x}{\bar{\gamma}_\mathrm{m}}\right)f_{|h_{sp}|^2}(y)dy}_{\Psi_1} \\ &+ \underbrace{\int_{\bar{\gamma}_\mathrm{th}/\bar{\gamma}_\mathrm{m}}^\infty F_{|h_{ss}|^2}\left(\frac{xy}{\bar{\gamma}_\mathrm{th}}\right)f_{|h_{sp}|^2}(y)dy}_{\Psi_2}. \end{aligned} \tag{13}$$

Referring to [19], we approximate the generalized-K PDF by a gamma PDF with a shape parameter m and a scale parameter ω for the convenience of derivation. As a result, $f_{|h_i|^2}(x)$ can be rewritten as

$$f_{|h_i|^2}(x) = \frac{x^{m-1}e^{-x/\omega}}{\omega^m\Gamma(m)},\ x>0 \tag{14}$$

where $m=\frac{\varepsilon\varphi}{\varepsilon+\varphi+1}$ and $\omega=\frac{\Omega_0}{m}$. Thus, we have

$$F_{|h_{ss}|^2}(x) = \frac{\gamma\left(m_{ss}, \frac{x}{\omega_{ss}}\right)}{\Gamma(m_{ss})} \tag{15}$$

where $\gamma(\cdot,\cdot)$ is the lower incomplete gamma function [20, Eq. (8.350.1)]. By substituting (15) into (13) and using the identity [20, Eq. (3.351.1)], we can get

$$\Psi_1 = \frac{\gamma\left(m_{sp}, \frac{\bar{\gamma}_\mathrm{th}}{\omega_{sp}\bar{\gamma}_\mathrm{m}}\right)}{\Gamma(m_{ss})\Gamma(m_{sp})}\gamma\left(m_{ss}, \frac{x}{\omega_{ss}\bar{\gamma}_\mathrm{m}}\right). \tag{16}$$

Similarly, we have

$$\Psi_2 = \int_{\bar{\gamma}_\mathrm{th}/\bar{\gamma}_\mathrm{m}}^\infty \frac{\gamma\left(m_{ss}, \frac{xy}{\omega_{ss}\bar{\gamma}_\mathrm{th}}\right)}{\Gamma(m_{ss})}\frac{y^{m_{sp}-1}e^{-\frac{y}{\omega_{sp}}}}{\omega_{sp}^{m_{sp}}\Gamma(m_{sp})}dy. \tag{17}$$

To derive the integral, we first expand $\gamma(\cdot,\cdot)$ according to [20, Eq. (8.352.1)], i.e.,

$$\frac{\gamma\left(m_{ss}, \frac{xy}{\omega_{ss}\bar{\gamma}_\mathrm{th}}\right)}{\Gamma(m_{ss})} = 1 - e^{-\frac{xy}{\omega_{ss}\bar{\gamma}_\mathrm{th}}}\sum_{i=0}^{m_{ss}-1}\frac{(xy)^i}{i!(\omega_{ss}\bar{\gamma}_\mathrm{th})^i}. \tag{18}$$

Then, by employing [20, Eq. (3.351.2)], the analytical expression for Ψ_2 is given by

$$\begin{aligned} \Psi_2 = &\frac{\Gamma\left(m_{sp}, \frac{\bar{\gamma}_\mathrm{th}}{\omega_{sp}\bar{\gamma}_\mathrm{m}}\right)}{\Gamma(m_{sp})} - \frac{1}{\omega_{sp}^{m_{sp}}\Gamma(m_{sp})}\sum_{i=0}^{m_{ss}-1}\frac{x^i}{i!(\omega_{ss}\bar{\gamma}_{th})^i} \\ &\times\left(\frac{1}{\omega_{sp}}+\frac{x}{\omega_{ss}\bar{\gamma}_\mathrm{th}}\right)^{-m_{sp}-i}\Gamma\left(m_{sp}+i, \frac{\bar{\gamma}_\mathrm{th}}{\omega_{sp}\bar{\gamma}_\mathrm{m}}+\frac{x}{\omega_{ss}\bar{\gamma}_\mathrm{m}}\right) \end{aligned} \tag{19}$$

where $\Gamma(\cdot,\cdot)$ is the upper incomplete gamma function [20, Eq. (8.350.2)]. Here, we define $C=\Gamma\left(m_{sp},\frac{\bar{\gamma}_{\rm th}}{\omega_{sp}\bar{\gamma}_{\rm m}}\right)\Big/\Gamma(m_{sp})$. From $\Gamma(1+n,x)+\gamma(1+n,x)=n!$, we obtain

$$\begin{aligned}F_{\bar{\gamma}_{\rm s}|h_{ss}|^2}(x)=1-\sum_{i=0}^{m_{ss}-1}\frac{(1-C)\,x^i}{i!\omega_{ss}^i\bar{\gamma}_{\rm m}^i}e^{\frac{x}{\omega_{ss}\bar{\gamma}_{\rm m}}}-\frac{1}{\omega_{sp}^{m_{sp}}\Gamma(m_{sp})}\\ \times\sum_{i=0}^{m_{ss}-1}\frac{x^i}{i!\left(\omega_{ss}\bar{\gamma}_{\rm th}\right)^i}\left(\frac{1}{\omega_{sp}}+\frac{x}{\omega_{ss}\bar{\gamma}_{\rm th}}\right)^{-m_{sp}-i}\\ \times\Gamma\left(m_{sp}+i,\frac{\bar{\gamma}_{\rm th}}{\omega_{sp}\bar{\gamma}_{\rm m}}+\frac{x}{\omega_{ss}\bar{\gamma}_{\rm m}}\right).\end{aligned}\tag{20}$$

Since in the considered network, the aggregate interference dominates the noise, $F_\gamma(x)$ can thus be approximated as

$$F_\gamma(x)\approx\int_0^\infty F_{\bar{\gamma}_{\rm s}|h_{ss}|^2}(xz)f_{\tilde{Z}}(z)\,dz.\tag{21}$$

By substituting (6) and (20) into (21) and express $\Gamma(\cdot,\cdot)$ with [20, Eq. (8.352.2)], we can further obtain

$$\begin{aligned}F_\gamma(x)=1-\frac{1-C}{\left(\bar{\gamma}_{\rm I}\tilde{\eta}_{\rm I}\right)^{k_{\rm I}}}\sum_{i=0}^{m_{ss}-1}\frac{(k_{\rm I})_i x^i}{i!\left(\bar{\gamma}_{\rm m}\omega_{ss}\right)^i}\left(\frac{1}{\bar{\gamma}_{\rm I}\tilde{\eta}_{\rm I}}+\frac{x}{\bar{\gamma}_{\rm m}\omega_{ss}}\right)^{-l}\\ -\frac{e^{-\bar{\gamma}_{\rm th}/(\bar{\gamma}_{\rm m}\omega_{sp})}}{\Gamma(k_{\rm I})\,\omega_{sp}^{m_{sp}}\left(\bar{\gamma}_{\rm I}\tilde{\eta}_{\rm I}\right)^{k_{\rm I}}}\sum_{i=0}^{m_{ss}-1}\frac{(m_{sp})_i x^i}{i!\left(\bar{\gamma}_{\rm th}\omega_{ss}\right)^i}\sum_{j=0}^{m_{sp}+i-1}\frac{\bar{\gamma}_{\rm th}^j}{j!\bar{\gamma}_{\rm m}^j}\\ \times\underbrace{\int_0^\infty e^{-\left(\frac{1}{\eta_{\rm I}}+\frac{x}{\bar{\gamma}_{\rm m}\omega_{ss}}\right)z}z^{l-1}\left(\frac{1}{\omega_{sp}}+\frac{xz}{\omega_{ss}\bar{\gamma}_{\rm th}}\right)^{-d}dz}_{J}\end{aligned}\tag{22}$$

where $l=k_{\rm I}+i$, $d=m_{sp}+i-j$. To solve the integral J, we express $\left(\frac{1}{\omega_{sp}}+\frac{xz}{\omega_{ss}\bar{\gamma}_{\rm th}}\right)^{-d}$ in terms of Meijer-j function [21, Eq. (10)], i.e.,

$$\left(\frac{1}{\omega_{sp}}+\frac{xz}{\omega_{ss}\bar{\gamma}_{\rm th}}\right)^{-d}=\frac{\omega_{sp}^d}{\Gamma(d)}G_{11}^{11}\left[\frac{\omega_{sp}xz}{\omega_{ss}\bar{\gamma}_{\rm th}}\,\middle|\,\begin{matrix}1-d\\0\end{matrix}\right].\tag{23}$$

For avoiding the Meijer-j function with two variables, we expand $e^{-\frac{xz}{\bar{\gamma}_{\rm m}\omega_{ss}}}$ into series with L terms and then using [20, Eq. (7.813.1)], we have

$$J=\frac{\omega_{sp}^d}{\Gamma(d)}\sum_{n=0}^{L}\frac{(-1)^n\left(\bar{\gamma}_{\rm I}\tilde{\eta}_{\rm I}\right)^{n+l}}{n!\left(\bar{\gamma}_{\rm m}\omega_{ss}\right)^n}x^nG_{21}^{12}\left[\frac{\omega_{sp}\bar{\gamma}_{\rm I}\tilde{\eta}_{\rm I}x}{\omega_{ss}\bar{\gamma}_{\rm th}}\,\middle|\,\begin{matrix}1-n-l,1-d\\0\end{matrix}\right].\tag{24}$$

From [20, Eq. (9.31.5)], $F_\gamma(x)$ can be simplified as

$$\begin{aligned}F_\gamma(x)=1-\frac{1-C}{\left(\bar{\gamma}_{\rm I}\tilde{\eta}_{\rm I}\right)^{k_{\rm I}}}\sum_{i=0}^{m_{ss}-1}\frac{(k_{\rm I})_i x^i}{i!\left(\bar{\gamma}_{\rm m}\omega_{ss}\right)^i}\left(\frac{1}{\bar{\gamma}_{\rm I}\tilde{\eta}_{\rm I}}+\frac{x}{\bar{\gamma}_{\rm m}\omega_{ss}}\right)^{-l}\\ -QG_{21}^{12}\left[\frac{\omega_{sp}\bar{\gamma}_{\rm I}\tilde{\eta}_{\rm I}}{\omega_{ss}\bar{\gamma}_{\rm th}}x\,\middle|\,\begin{matrix}1-k_{\rm I},1-d\\n+i\end{matrix}\right]\end{aligned}\tag{25}$$

with

$$Q=\frac{e^{-\frac{\bar{\gamma}_{\rm th}}{\bar{\gamma}_{\rm m}\omega_{sp}}}}{\Gamma(k_{\rm I})}\sum_{i=0}^{m_{ss}-1}\frac{(m_{sp})_i}{i!}\sum_{j=0}^{m_{sp}+i-1}\frac{1}{j!\Gamma(d)\,\bar{\gamma}_{\rm m}^j}\sum_{n=0}^{L}\frac{(-1)^n\bar{\gamma}_{\rm th}^{j+n}}{\left(\bar{\gamma}_{\rm m}\omega_{sp}\right)^{j+n}}$$

TABLE I
GENERALIZED-K CHANNEL PARAMETERS [17].

Shadowing	σ	φ	ε
Infrequent light shadowing (ILS)	0.161	38.0809	2.5
Average shadowing (AS)	0.345	7.9115	2.5
Frequent heavy shadowing (FHS)	0.806	1.0931	2.5

where $(u)_v=\frac{\Gamma(u+v)}{\Gamma(u)}$ is a pochhammer symbol. Then, the analytical expression for $M_\gamma(s)$ in (10) can be obtained as

$$\begin{aligned}M_\gamma(s)=s^{-2}-\sum_{i=0}^{m_{ss}-1}\frac{1-C}{\Gamma(k_{\rm I})\,i!}G_{12}^{21}\left[\frac{\bar{\gamma}_{\rm m}\omega_{ss}}{\bar{\gamma}_{\rm I}\tilde{\eta}_{\rm I}}s\,\middle|\,\begin{matrix}1-i\\1,k_{\rm I}\end{matrix}\right]\\ -QG_{13}^{31}\left[\frac{\omega_{ss}\bar{\gamma}_{\rm th}s}{\omega_{sp}\bar{\gamma}_{\rm I}\tilde{\eta}_{\rm I}}\,\middle|\,\begin{matrix}1-n-i\\1,k_{\rm I},m_{sp}-n-j\end{matrix}\right].\end{aligned}\tag{26}$$

Finally, by substituting (26) into (10) and employing [20, Eq. (7.813.1)], the effective capacity can be derived as

$$\begin{aligned}E_c(\theta)=-\frac{1}{\beta\ln 2}\ln\left(\frac{\Gamma(\beta-2)}{\Gamma(\beta)}-\sum_{i=0}^{m_{ss}-1}\frac{1-C}{\Gamma(k_{\rm I})\,i!\Gamma(\beta)}\right.\\ \times G_{22}^{22}\left[\frac{\bar{\gamma}_{\rm m}\omega_{ss}}{\bar{\gamma}_{\rm I}\tilde{\eta}_{\rm I}}\,\middle|\,\begin{matrix}1-\beta,1-i\\1,k_{\rm I}\end{matrix}\right]\\ \left.-\frac{Q}{\Gamma(\beta)}G_{23}^{32}\left[\frac{\omega_{ss}\bar{\gamma}_{\rm th}}{\omega_{sp}\bar{\gamma}_{\rm I}\tilde{\eta}_{\rm I}}\,\middle|\,\begin{matrix}1-\beta,1-n-i\\1,k_{\rm I},m_{sp}-n-j\end{matrix}\right]\right).\end{aligned}\tag{27}$$

IV. Results and Analysis

In this section, numerical simulations are conducted to corroborate our theoretical results and characterize the effects of different system parameters on the effective capacity of satellite communications. In the simulations, we set the block length $T_f=2$ ms, system bandwidth $B=100$ KHz, outer radius R=10 Km and radius of exclusion region $r=2$ Km.

In the considered network, satellite downlinks are modeled as generalized-K distributions with $\Omega_0=1$ and $\varepsilon=2.5$. The detailed channel parameters are given in Table I, where σ is the standard deviation of the log-normal shadowing and increases as the amount of fading increases. Using a moment matching technique [19], the corresponding parameter φ of the generalized-K distribution can be linked to $\varphi=\frac{1}{e^{\sigma^2}-1}$. We consider three shadowing cases in this paper, infrequent light shadowing (ILS), average shadowing (AS), and frequent heavy shadowing (FHS). Specifically, the interference link h_{sp} experiences AS shadowing, while the communication link h_{ss} is assumed to experience three shadowing cases respectively. For terrestrial links, we set $k_{ps}=2$ and $\eta_{ps}=0.5$.

Fig. 2 performs the normalized effective capacity of satellite systems for various fading cases with INR $=0,5$. It can be seen that the effective capacity consistently decreases when the shadowing or the interference power increases, both of which deteriorate the received SINR at the FSS terminal and thus the transmission rate. Moreover, the theoretical curves are obtained using (27) with $L=30$. We can observe

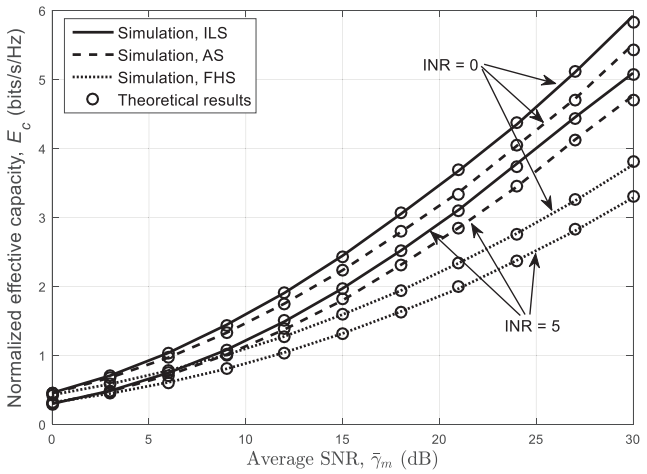

Fig. 2. Normalized effective capacities of satellite systems for different INRs with $\bar{\gamma}_{\rm m} = \bar{\gamma}_{\rm th}$ and h_{ss} experiencing various shadowing cases ($\lambda = 0.5$, $\alpha = 3$, $\theta = 10^{-2}$).

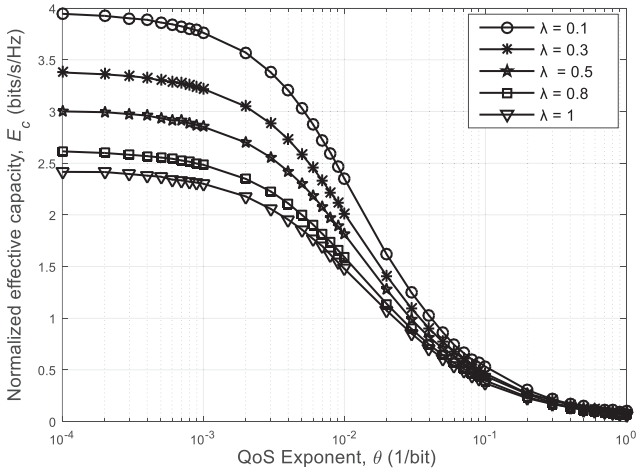

Fig. 4. Simulated normalized effective capacities versus QoS exponent for various intensities of PPP with h_{ss} experiencing AS shadowing ($\bar{\gamma}_{\rm m} = \bar{\gamma}_{\rm th} =$ 15 dB, INR $= 5$ dB, $\alpha = 3$).

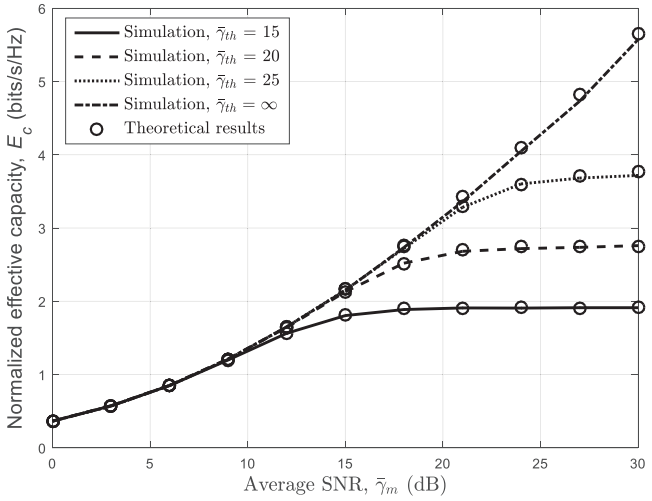

Fig. 3. Normalized effective capacities of satellite systems for different interference-power constraints $\bar{\gamma}_{\rm th}$ with h_{ss} experiencing AS shadowing (INR $= 5$ dB, $\lambda = 0.5$, $\alpha = 3$, $\theta = 10^{-2}$).

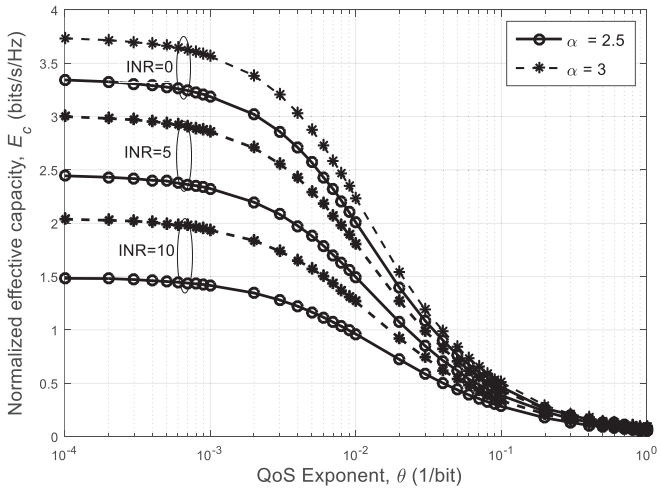

Fig. 5. Simulated normalized effective capacities versus QoS exponent for various path-loss exponents and INRs with h_{ss} experiencing AS shadowing ($\bar{\gamma}_{\rm m} = \bar{\gamma}_{\rm th} = 15$ dB, $\lambda = 0.5$).

that the theoretical results agree well with the Monte Carlo simulations, confirming the accuracy of our analysis.

Fig. 3 depicts the normalized effective capacity for various $\bar{\gamma}_{\rm th}$, illustrating the impact of different interference-power limitations on the performance of satellite systems. As observed, the effective capacity under an interference-power constraint is inferior compared to the system with no interference-power constraint (i.e., $\bar{\gamma}_{\rm th} = \infty$). Moreover, the looser the interference-power constraint is, i.e., $\bar{\gamma}_{\rm th}$ gets larger, the higher the effective capacity is. Besides, due to the existence of interference-power constraints, the effective capacity of satellite systems becomes saturated eventually. These phenomena indicate that for the coexistence of the satellite and terrestrial systems, there is a balance between the performance of two systems.

Fig. 4 and Fig. 5 present the normalized effective capacity of satellite systems versus the delay QoS exponent θ for various terrestrial interfering parameters such as intensity of PPP λ, average INR, and interference link quality (i.e., path-loss exponent α). Firstly, both figures show that effective capacity decreases upon increasing QoS exponent θ, which means as the delay constraint becomes more critical, the less effective rate the system can support. Moreover, from Fig. 4 we can find that the effective capacity decreases as λ increases, which relates to the number of interference links in a finite area. It is interesting to note that as λ decreases from 1 to 0.1, the gap between the corresponding curves increases, which implies that its effect becomes more pronounced. Similarly, Fig. 5 illustrates that when the intensity of PTs is certain, the effective capacity decreases as either the average INR or the quality of interference link increases, both of which determine

the received interference power from each PT.

V. Conclusions

In this paper, we have considered an underlay cognitive satellite-terrestrial network where the satellite communication operates in the microwave frequency bands allocated to terrestrial networks. Taking the statistical delay QoS requirements into account, we have investigated the effective capacity of the satellite network while satisfying the interference-power limitations of the terrestrial network. By characterizing the aggregate interference caused by PPP based primary transmitters, we have derived the exact expression for the effective capacity in a closed-form, the validity of which has been confirmed by Monte Carlo simulations. Our study has revealed that for the coexistence of the satellite and terrestrial systems, there is a balance between the performance of two systems.

VI. Acknowledgement

The authors would like to acknowledge the support from the International S&T Cooperation Program of China (No. 2014DFA11640), EU H2020 ITN 5G Wireless project (Grant No. 641985), EU FP7 QUICK project (Grant No. PIRSES-GA-2013-612652), EPSRC TOUCAN project (Grant No. EP/L020009/1), the 111 Project (B08038), and the National Key Research and Development Program of China (2016YFB1200202).

References

[1] S. Kandeepan, L. De Nardis, M. G. Di Benedetto, A. Guidotti, and G. E. Corazza, "Cognitive satellite terrestrial radios," in *Proc. IEEE GLOBECOM'10*, Miami, USA, Dec. 2010, pp. 1–6.

[2] M. Hyhty, J. Kyrlinen, A. Hulkkonen, J. Ylitalo, and A. Roivainen, "Application of cognitive radio techniques to satellite communication," in *Proc. DYSPAN'12*, Bellevue, USA, Oct. 2012, pp. 540–551.

[3] S. K. Sharma, S. Chatzinotas, and B. Ottersten, "Satellite cognitive communications: Interference modeling and techniques selection," in *6th ASMS and SPSC*, Baiona, Spain, Sep. 2012, pp. 111–118.

[4] E. Lagunas, S. K. Sharma, S. Maleki, S. Chatzinotas, and B. Ottersten, "Resource allocation for cognitive satellite communications with incumbent terrestrial networks," *IEEE Trans. Cognitive Commun. Networking*, vol. 1, no. 3, pp. 305–317, Sep. 2015.

[5] F. Guidolin, M. Nekovee, L. Badia, and M. Zorzi, "A cooperative scheduling algorithm for the coexistence of fixed satellite services and 5G cellular network," in *Proc. IEEE ICC'15*, London, UK, June 2015, pp. 1322–1327.

[6] S. Vassaki, M. I. Poulakis, A. D. Panagopoulos, and P. Constantinou, "Power allocation in cognitive satellite terrestrial networks with QoS constraints," *IEEE Commun. Lett.*, vol. 17, no. 7, pp. 1344–1347, Jul. 2013.

[7] K. An, J. Ouyang, M. Lin, and T. Liang, "Outage analysis of multi-antenna cognitive hybrid satellite-terrestrial relay networks with beamforming," *IEEE Commun. Lett.*, vol. 19, no. 7, pp. 1157–1160, Jul. 2015.

[8] C. Niephaus, M. Kretschmer, and G. Ghinea, "QoS provisioning in converged satellite and terrestrial networks: A survey of the state-of-the-art," *IEEE Commun. Surveys & Tutorials*, in press.

[9] Z. Ji, Y. Wang, W. Feng, and J. Lu, "Delay-aware power and bandwidth allocation for multiuser satellite downlinks," *IEEE Commun. Lett.*, vol. 18, no. 11, pp. 1951–1954, Nov. 2014.

[10] S. Vassaki, A. D. Panagopoulos, and P. Constantinou, "Effective capacity and optimal power allocation for mobile satellite systems and services," *IEEE Commun. Lett.*, vol. 16, no. 1, pp. 60–63, Jan. 2012.

[11] Dapeng Wu and R. Negi, "Effective capacity: a wireless link model for support of quality of service," *IEEE Trans. Wireless Commun.*, vol. 2, no. 4, pp. 630–643, July 2003.

[12] P. C. Pinto and M. Z. Win, "Communication in a poisson field of interferers–Part I: Interference distribution and error probability," *IEEE Trans. Wireless Commun.*, vol. 9, no. 7, pp. 2176–2186, July 2010.

[13] S. Maleki *et al*., "Cognitive spectrum utilization in Ka band multibeam satellite communications," *IEEE Commun. Mag.*, vol. 53, no. 3, pp. 24–29, Mar. 2015.

[14] S. Kusaladharma and C. Tellambura, "Aggregate interference analysis for underlay cognitive radio networks," *IEEE Wireless Commun. Lett.*, vol. 1, no. 6, pp. 641–644, Dec. 2012.

[15] A. Abdi, W. Lau, M. S. Alouini, and M. Kaveh, "A new simple model for land mobile satellite channels: first and second order statistics," *IEEE Trans. Wireless Commun.*, vol. 2, no. 3, pp. 519–528, May 2003.

[16] G. N. Kamga, M. Xia, and S. Aissa, "A unified performance evaluation of integrated mobile satellite systems with ancillary terrestrial component," in *Proc. IEEE ICC'15*, London, UK, June 2015, pp. 934–938.

[17] K. P. Peppas, "Accurate closed-form approximations to generalised-K sum distributions and applications in the performance analysis of equal-gain combining receivers," *IET Commun.*, vol. 5, no. 7, pp. 982–989, May 2011.

[18] Z. Ji, C. Dong, Y. Wang, and J. Lu, "On the analysis of effective capacity over generalized fading channels," in *Proc. IEEE ICC'14*, Sydney, Australia, June 2014, pp. 1977–1983.

[19] S. Al-Ahmadi and H. Yanikomeroglu, "On the approximation of the generalized-K distribution by a gamma distribution for modeling composite fading channels," *IEEE Trans. Wireless Commun*., vol. 9, no. 2, pp. 706–713, Feb. 2010.

[20] I. S. Gradshteyn and I. M. Ryzhik, *Table of Integrals, Series, and Products*, 6th ed. Academic Press, 2000.

[21] V. S. Adamchik and O. I. Marichev, "The algorithm for calculating integrals of hypergeometric type functions and its realization in reduce systems" in *Proc. Int. Conf. Symp. Algebraic Comput.*, Tokyo, Japan, 1990, pp. 212–224.